

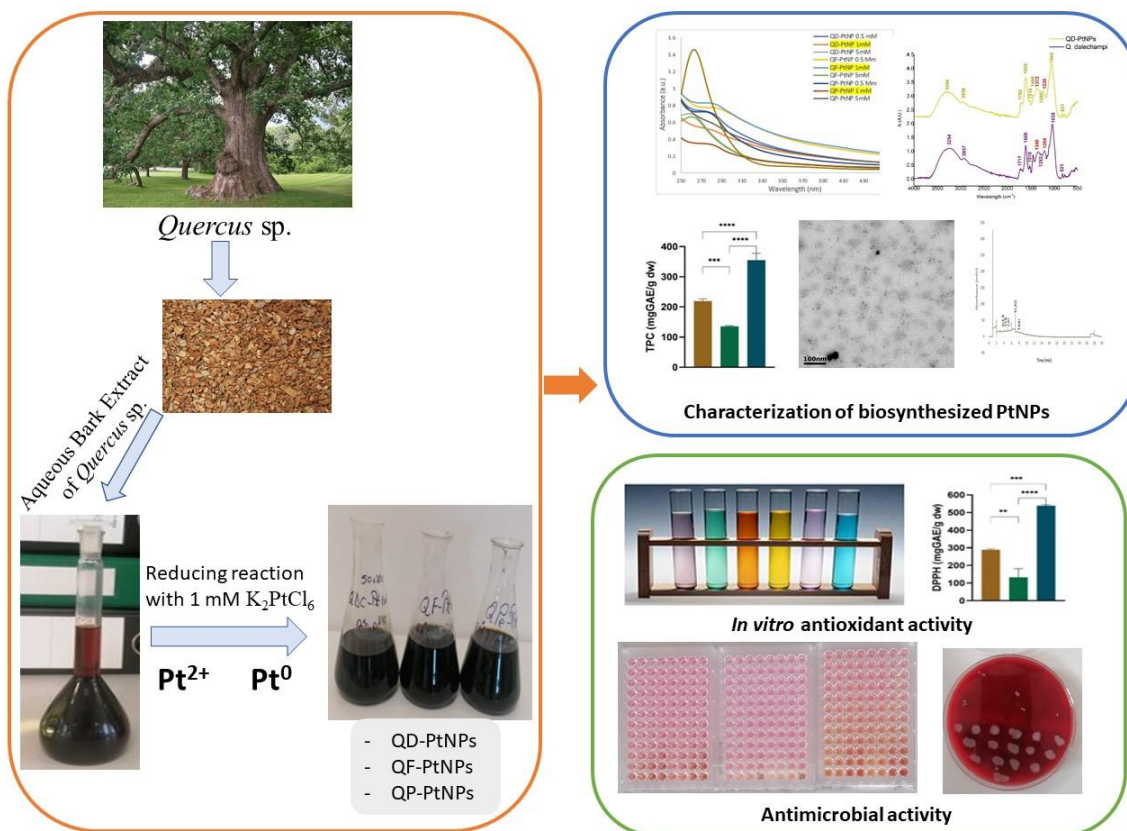
# Green Synthesis of Platinum Nanoparticles Using Aqueous Bark Extract of *Quercus* sp. for Potential Antioxidant and Antimicrobial Applications

Năstaca-Alina Coman,<sup>a</sup> Lavinia Berta,<sup>b,\*</sup> Alexandra Nicolae-Maranciuc,<sup>c,d</sup> Alexandru Nicolescu,<sup>e</sup> Mihai Babotă,<sup>e,f</sup> Adrian Man,<sup>g</sup> Dan Chicea,<sup>c</sup> Lenard Farczadi,<sup>h</sup> László Jakab-Farkas,<sup>i</sup> and Corneliu Tanase<sup>f,j</sup>

DOI: 10.15376/biores.19.4.8621-8641

\*Corresponding author: [lavinia.bera@umfst.ro](mailto:lavinia.bera@umfst.ro)

## GRAPHICAL ABSTRACT



# Green Synthesis of Platinum Nanoparticles Using Aqueous Bark Extract of *Quercus* sp. for Potential Antioxidant and Antimicrobial Applications

Năstaca-Alina Coman,<sup>a</sup> Lavinia Berta,<sup>b,\*</sup> Alexandra Nicolae-Maranciuc,<sup>c,d</sup> Alexandru Nicolescu,<sup>e</sup> Mihai Babotă,<sup>e,f</sup> Adrian Man,<sup>g</sup> Dan Chicea,<sup>c</sup> Lenard Farczadi,<sup>h</sup> László Jakab-Farkas,<sup>i</sup> and Corneliu Tanase<sup>f,j</sup>

Oak bark, which is commonly used in the wood industry, has by-products often repurposed as fuel. Its extracts are rich in compounds with anticancer, antibacterial, antifungal, and anti-inflammatory properties. This study synthesized platinum nanoparticles (PtNPs) using aqueous extracts from *Quercus dalechampii* (QD), *Q. frainetto* (QF), and *Q. petraea* (QP). Key factors during nanoparticle formation included reaction time, metal ion concentration, pH, extract-to-metal ion ratio, and temperature. The PtNPs were characterized by dynamic light scattering, Fourier transform infrared spectroscopy, and transmission electron microscopy. The average diameters were  $58.5 \pm 7.6$  nm for QD-PtNPs,  $41.6 \pm 5.4$  nm for QF-PtNPs, and  $41 \pm 5.3$  nm for QP-PtNPs. Antioxidant and antimicrobial activities were also analyzed. The QP-PtNPs had the highest DPPH (2,2-Diphenyl-1-picrylhydrazyl), FRAP (Ferric Reducing Antioxidant Power), and CUPRAC (Cupric Reducing Antioxidant Capacity) free radical scavenging activities, while QD-PtNPs excelled in ABTS (2,2'-azino-bis-(3-ethylbenzothiazoline-6-sulfonic acid)) scavenging. All PtNPs showed strong antimicrobial properties, particularly against *Enterococcus faecalis*, *Escherichia coli*, *Candida krusei*, and *Candida auris*. These findings suggest that *Quercus*-mediated PtNPs have significant potential for developing treatments against bacterial and fungal infections, with promising applications in medicine.

DOI: 10.15376/biores.19.4.8621-8641

**Keywords:** Biosynthesis; Platinum nanoparticles; *Quercus*; Rhytidome; Phenolic compounds; Antioxidant activity; Antibacterial activity; Antifungal activity

**Contact information:** a: Doctoral School of Medicine and Pharmacy, “George Emil Palade” University of Medicine, Pharmacy, Sciences and Technology of Târgu Mures, Târgu Mures, Romania; b: Department of General and Inorganic Chemistry, “George Emil Palade” University of Medicine, Pharmacy, Sciences and Technology of Târgu Mureş, 540139 Târgu Mureş, Romania; c: Research Center for Complex Physical Systems, Faculty of Sciences, Lucian Blaga University of Sibiu, 550012 Sibiu, Romania; d: Institute for Interdisciplinary Studies and Research (ISCI), Lucian Blaga University of Sibiu, 550024 Sibiu, Romania; e: Department of Pharmaceutical Botany, Faculty of Pharmacy, “Iuliu Hatieganu” University of Medicine and Pharmacy, 400337 Cluj-Napoca, Romania; f: Research Center of Medicinal and Aromatic Plants, “George Emil Palade” University of Medicine, Pharmacy, Sciences and Technology of Târgu Mures, 540139 Târgu Mures, Romania; g: Department of Microbiology, Faculty of Medicine, “George Emil Palade” University of Medicine, Pharmacy, Sciences and Technology of Târgu Mures, 540139 Târgu Mures, Romania; h: Chromatography and Mass Spectrometry Laboratory, Center for Advanced Medical and Pharmaceutical Research, “George Emil Palade” University of Medicine, Pharmacy, Sciences and Technology of Târgu Mures, 540139 Târgu Mures, Romania; i: Faculty of Technical and Human Sciences, Sapientia Hungarian University of Transylvania, 540485 Târgu Mureş, Romania; j: Department of Pharmaceutical Botany, Faculty of Pharmacy, “George Emil Palade” University of Medicine, Pharmacy, Sciences and Technology of Târgu Mures, 540139 Târgu Mures, Romania;

\*Corresponding author: [lavinia.bertha@umfst.ro](mailto:lavinia.bertha@umfst.ro)

## INTRODUCTION

In recent years, there has been a growing interest in the formation of platinum nanoparticles (PtNPs) (Bhardwaj *et al.* 2020) due to their ability to fight bacteria (Eltaweil *et al.* 2022), as well as their anticancer (Bendale *et al.* 2017), catalytic (Karim *et al.* 2019), and antioxidant effects (Gupta and Chundawat 2019). Conventional techniques for their production usually require chemical procedures that involve high energy consumption or the use of harmful substances. Furthermore, PtNPs have been utilized in the creation of chemotherapy medications, such as carboplatin, cisplatin, and oxaliplatin, which are administered for treating forms of cancers such as ovarian cancer (Zeeshan *et al.* 2014). Nevertheless, these medications often lead to adverse effects in patients including kidney damage, nerve damage, and cell toxicity (Bendale *et al.* 2017). These adverse effects could potentially be mitigated by utilizing a biosynthesis method for producing PtNPs. The biosynthesis process of PtNPs mainly involves plants, bacteria, and fungi. The synthesis of metal nanoparticles from plant extracts is preferred, because it is faster and more ecological than that from fungi and bacteria (Siddiqi *et al.* 2018). The presence of flavonoids, protein-amine residues, and carboxylic acids in plants play a role, in reducing platinum ions to form PtNPs (Castro *et al.* 2015). Biosynthesized PtNPs have many advantages, they are used in different fields, especially the pharmaceutical and biomedical fields, because of their compatibility with living organisms, ecological sustainability, and cost-effectiveness (Jiao *et al.* 2021; Zhang *et al.* 2023). Platinum nanoparticles (PtNPs) synthesized through green methods have demonstrated remarkable efficiency in inhibiting the growth of bacterial pathogens (Dhiman *et al.* 2021). For instance, the synthesis of PtNPs using extracts from *Citrus hystrix* DC., *Ocimum basilicum* Linn., and *Pandanus amaryllifolius* Roxb. produced nanoparticles with spherical morphologies and sizes ranging from 20 to 80 nm (Ponsanti *et al.* 2024). Recently, it has been shown that the peroxidase-like catalytic activity of PtNPs can be utilized for colorimetric detection methods of biomarkers, with a detection limit of 7.00  $\mu\text{M}$  (Marvi *et al.* 2024). Additionally, PtNPs synthesized using extracts from *Salvia rosmarinus* and *Panax ginseng* have induced cell death in colon cancer cell lines, with PCR analysis of autophagy and apoptosis markers indicating a significant influence of the nanoparticles (Alinaghi *et al.* 2024). These examples highlight the considerable potential of PtNPs synthesized through green methods in biomedical and diagnostic applications, thereby underscoring the importance of our research in using *Quercus* extracts for the synthesis and stabilization of these nanoparticles.

Oak bark, sourced from *Quercus dalechampii* (QD), *Q. frainetto* (QF), and *Q. petraea* (QP) trees, are commonly utilized in the timber sector with their byproducts often repurposed for fuel (Tanase *et al.* 2023; Tsiripidis and Athanasiadis 2003).

To our knowledge, there is no evidence that extracts of *Q. dalechampii*, *Q. frainetto*, and *Q. petraea* have been used to synthesize platinum nanoparticles (PtNPs). In a previously published study, the authors demonstrated that oak bark extract is rich in polyphenols and flavonoids, having remarkable antibacterial and antifungal properties (Coman *et al.* 2024). This suggests that the use of this extract for the biosynthesis of PtNPs could lead to nanoparticles with activity significant antimicrobial. Additionally, oak bark is an abundant and sustainable material, making its use in nanoparticle synthesis both environmentally friendly and cost-effective. By highlighting these distinctive aspects of oak bark extract, the aim here is to emphasize the importance and relevance of this study in the current context of nanoparticle research. Thus, the main objectives of this study were: (1) biosynthesis of PtNPs using oak bark extracts as a natural resource; (2) to investigate the impact of key factors on the biosynthesis process of PtNPs, including variations in the

concentration of H<sub>2</sub>PtCl<sub>6</sub> (0.5, 1.0, and 5 mM), pH levels (7.5, 8, 9, and 10), the ratio of bark extract to H<sub>2</sub>PtCl<sub>6</sub> (1:9, 2:8, 1:19), and temperature fluctuations (50 °C, 70 °C and 80 °C); (3) characterization of biosynthesized PtNPs by specific analyses; and (4) evaluate the antioxidant, antibacterial, and antifungal properties of the synthesized PtNPs.

## EXPERIMENTAL

### Plant Material

Bark fragments of *Q. dalechampii*, *Q. frainetto*, and *Q. petraea* were collected from mature trees (35 to 40 years old, 18 to 25 cm circumference at breast height) from the Zagra area of Bistrița Năsăud county, Romania. The species' authenticity was confirmed by Dr. Corneliu Tănase from the Department of Pharmaceutical Botany at the Faculty of Pharmacy G. Emil Palade University of Medicine and Pharmacy, Târgu Mureș, Romania. The collected bark was air dried in a Nahita 631 drying oven at 50 °C for a day. Then, it was pulverized using a Pulverisette 15 cutting mill from Fritsch GmbH, Idar Oberstein, Germany. This powdered material was left unprocessed and deposited in the Research Center for Medicinal and Aromatic Plants, Târgu Mureș, Romania until further extraction procedures were performed.

### Chemicals and Reagents

Potassium hexachloroplatinate(II) hexahydrate (K<sub>2</sub>PtCl<sub>6</sub>·6H<sub>2</sub>O, 99.9%), sodium hydroxide (NaOH), DPPH (2,2-diphenyl-1-picrylhydrazyl), ABTS (2,2'-azinobis(3-ethylbenzothiazoline-6-sulfonic acid)), FRAP (Ferric Reducing Ability of Plasma), CUPRAC (Cupric Ion Reducing Antioxidant Capacity), NR (neutral red) solutions were purchased from Sigma-Aldrich in Steinheim, Germany. Dimethyl sulfoxide (DMSO), and Folin-Ciocalteu reagent were obtained from Merck (Darmstadt, Germany).

### Microorganisms

*Staphylococcus aureus* ATCC 25923 and ATCC 43300, *Enterococcus faecalis* ATCC 29212, *Escherichia coli* ATCC 25922, *Klebsiella pneumoniae* ATCC 13883, *Pseudomonas aeruginosa* ATCC 27853, *Candida albicans* ATCC 10213, *Candida krusei* ATCC 6258, and *Candida auris* ATCC 10913 were obtained from the Department of Microbiology at the University of Medicine, Pharmacy, Sciences and Technology "George Emil Palade", Târgu Mureș, Romania.

### Preparation of Bark Extracts

Extraction was performed with distilled water at a ratio of 1:10, as previously described (Tanase *et al.* 2020). In short, 10 g of oak bark was put in a flask with 100 mL of water, ensuring thorough saturation of the plant material. The extraction process was conducted at a temperature of 60 °C for 30 min. Polyphenolic substances were obtained using an ultrasonic water bath (Professional Ultrasonic Cleaner MRC from Beijing, China) with the following settings: AC 150 H, 150 W, 40 kHz, and heating power 300 W. After extraction, the resulting extracts were filtered and centrifuged at a speed of 10,000 revolutions/min for about 10 min. The supernatant was used for the experiment. The extracts were used directly without any processing for the synthesis of PtNPs.

## Chemical Characterization of Bark Extracts

### *Qualitative analysis of bark extracts*

An UHPLC analysis (Ultra-High-Performance Liquid Chromatography) of the polyphenolic compounds was detailed by Tanase *et al.* (2018). The analysis utilized a Perkin Elmer UPLC Flexar FX 10 system, which included components, like a pump, inline degasser, autosampler, column thermostat, and a Flexar FX PDA UHPLC detector. High quality liquid chromatography-mass spectrometry (LC-MS)/MS grade solvents and the purest reagents available were used throughout the process. Samples were injected into a Luna C18 (2) column (3  $\mu\text{m}$  particle size, 150 mm  $\times$  4.6 mm) at a flow rate of 1.0 mL/min. Elution was carried out using a gradient of 0.1% formic acid (phase A) and acetonitrile (phase B) with monitoring at 280 nm. Compound identification was achieved by comparing retention times and ultraviolet-visible (UV-Vis) spectra with reference standards. Before analysis all extracts underwent filtration through a 0.45- $\mu\text{m}$  microporous cellulose syringe filter. UHPLC was used both to identify and quantify specific compounds from the extracts used and to identify and quantify the compounds remaining after the synthesis of PtNPs. It is important to determine the chemical composition of the extract and to understand how these compounds influence the synthesis and properties of the nanoparticles.

### Quantitative Analysis of Bark Extracts

The method used to calculate total polyphenol content (TPC) from extracts and from nanoparticles followed the Folin Ciocalteu method adapted for the microplate reader, as described by Babota *et al.* (2021). The absorbance of the samples was measured at 760 nm after a 30 min incubation at room temperature. Results are expressed in mg gallic acid equivalents (GAE) per gram weight (dw) of lyophilized extract/nanoparticles (mg GAE/g dw). Gallic acid was used as a standard and each sample was measured in triplicate.

### Biosynthesis of PtNPs Using Polyphenolic Extracts

The synthesis of PtNPs was monitored and optimized by recording the UV-Vis spectra of the reaction mixtures in the wavelength range of 250 to 450 nm (Tanase *et al.* 2019) on a Specord 210 Plus 190 spectrophotometer (Analytik Jena, Jena, Thuringia, Germany). To enhance the production efficiency of PtNPs, various parameters were adjusted during the synthesis, including the pH levels (7.5, 8, 9, and 10),  $\text{H}_2\text{PtCl}_6$  concentration (0.5, 1.0, and 5 mM), ratio of bark extract to  $\text{H}_2\text{PtCl}_6$  (1:9, 2:8, 1:19), temperature variations (50, 70, and 80  $^\circ\text{C}$ ) and different reaction durations (30, 60, 90, and 120 min). The pH level was regulated using NaOH solution at a concentration of 1.0 mM. After finishing the optimization studies, the synthesis of PtNPs was performed using the optimal parameters. The solutions of QD-PtNPs, QF-PtNPs, and QP-PtNPs were freeze dried using a BK-FD12S freeze dryer (Biobase Biodustry Co., Ltd., Shandong, China). The pellets of QD-PtNPs, QF-PtNPs, and QP-PtNPs were then stored at +4  $^\circ\text{C}$  until use.

### Characterization of PtNPs

The PtNPs were examined using Fourier transform infrared spectroscopy (FTIR), dynamic light scattering (DLS), and transmission electron microscopy (TEM). Attenuated total reflectance-FTIR (ATR-FTIR) spectroscopy (Bruker Alpha-P ATR FTIR spectrometer, Bruker, Ettlingen, Germany) was used to identify functional groups on the surface of PtNPs, which are part of compounds found in bark extracts that serve as coating or stabilizing agents. Briefly, the freeze-dried extracts and PtNPs pellets were subjected to ATR-FTIR spectroscopy in the range of 4000 to 400  $\text{cm}^{-1}$  with a resolution of 4  $\text{cm}^{-1}$  (Chicea *et al.* 2023). The morphology and size of the PtNPs were studied through TEM

and DLS analyses. Thus, PtNPs solution was used for TEM and DLS analyses. Briefly, for TEM analysis, a drop of each PtNPs was placed on carbon coated copper grids (300 mesh). The specimens were vacuum dried for 24 h, at room temperature (Tanase *et al.* 2019). The size of the synthesized PtNPs was determined using DLS, where a beam of light is directed at particles suspended in a solvent to generate patterns that are captured by a detector (Chicea *et al.* 2024).

### Assessment of Antioxidant Activity for PtNPs

The antioxidant potential of synthesized PtNPs was evaluated by DPPH, ABTS, FRAP, and CUPRAC reagents using the procedures described by Babota *et al.* (2022) and Mocan *et al.* (2016). The QD-PtNPs, QF-PtNPs, and QP-PtNPs were dissolved in a mixture of 50% ethanol with 5% DMSO to obtain a concentration of 1.0 mg/mL, which was then further diluted. Subsequently, samples were assessed in 96 well plates using a SPECTROstar® Nano Multi-Detection microplate reader, from BMG Labtech located in Ortenberg, Germany.

#### DPPH radical scavenging assay

This assay involved mixing 30  $\mu$ L of each sample with a 0.004% methanol solution of 1,1-diphenyl-2-picrylhydrazyl reagent. After an incubation period of 30 min, at room temperature in the dark the absorbance was measured at 517 nm. The outcomes of DPPH scavenging activity were reported as mg of Trolox equivalents per gram of freeze-dried powder (mg TE/g dw) (Babotă *et al.* 2018).

#### ABTS radical scavenging assay

A 7 mM 2,2'-azino-bis(3-ethylbenzothiazoline) 6-sulfonic acid solution was mixed with 2.45 mM potassium persulfate. It was left to stand in the dark at room temperature for 12 to 16 h. Before conducting the test, the ABTS solution was diluted with water until it reached an absorbance of  $0.700 \pm 0.02$  at 734 nm. The diluted samples were then combined with the ABTS solution. Then, it was mixed thoroughly. After a 30 min incubation period at room temperature, the absorbances of the samples were measured at 734 nm. The results of the ABTS scavenging activity were reported as milligrams of Trolox equivalents, per gram of freeze-dried powder (mg TE/g dw).

#### FRAP activity

The ferric reducing antioxidant power testing was accomplished through the combination of 25  $\mu$ L of the sample with 175  $\mu$ L of the FRAP reagent. The resulting mixture was left to incubate for 30 min at room temperature, following which the absorbance was measured at 593 nm. The prepared FRAP reagent consisted of a blend of buffer (300 mM, pH 3.6) TPTZ solution (10 mM TPTZ in 40 mM HCl), and FeCl<sub>3</sub> solution (20 mM FeCl<sub>3</sub>·6H<sub>2</sub>O in 40 mM HCl) in specific proportions. The outcomes were stated as milligrams of Trolox equivalents, per gram of freeze-dried powder (mg TE/g dw).

#### CUPRAC assay

A modified protocol of previously reported method (Özyürek *et al.* 2011) was used. During this process each sample was mixed with a solution containing CuCl<sub>2</sub>, neocuproine, and ammonium acetate at a pH level of 7.0. Following a 30 min waiting period the absorbance of the mixture was gauged at 450 nm. The findings were then expressed as milligrams of Trolox equivalents, per gram of freeze-dried powder (mg TE/g dw).

## Assessment of Antimicrobial Activity for PtNPs

The effectiveness of QD-PtNPs, QF-PtNPs, and QP-PtNPs, against bacteria was assessed through the microdilution technique following a previously described method (Tanase *et al.* 2018; Coman *et al.* 2023) with slight modifications. The study measured the efficacy of PtNPs pellets by determining minimum inhibitory concentration (MIC, required for microbial growth inhibition) and fungicidal concentrations (MFC) using a method known as microdilution. Briefly, 150 mg of lyophilized material was mixed with 15 mL of 5% DMSO solution (concentration of 10 mg/mL). After, 200  $\mu$ L of this solution was added to the wells of the first column of a 96-well plate. The solutions were then diluted using distilled water (final volume 100  $\mu$ L) followed by the addition of 100  $\mu$ L of bacterial / fungicidal suspension to each well. Each substance and bacterial/fungal strain were tested three times for accuracy. The microdilution plates were placed in an incubator at 37 °C for a period of 24 h. The MIC or MFC were assessed in wells where there was no bacterial growth or fungal growth by optical examination.

## Statistical Analysis

Statistical analysis was performed with GraphPad Prism 8 (GraphPad Software, San Diego, CA, USA). The significance level chosen was  $\alpha = 0.05$ . The normality of data distribution was checked using the Shapiro-Wilk test. The TPC and antioxidant activity was performed using the one-way analysis of variance (ANOVA) test, and Tukey's *post hoc* test was used to compare groups. Any p value < 0.05 was considered significant.

## RESULTS AND DISCUSSION

### Chemical Characterization of Bark Extracts

The aqueous extracts obtained were characterized by UV-Vis spectroscopy (Fig. 1a). The maximum absorption for the *Q. dalechampii* extract was at 272 nm, for the *Q. frainetto* extract at 277 nm, and for the *Q. petraea* extract at 274 nm. The aqueous extracts were also examined to determine the total content of phenolic compounds (TPC) and the specific components present in the extracts. As a result, *Q. dalechampii* showed a TPC value of 402 mg GAE/g extract, while *Q. frainetto* showed 438 mg GAE/g extract, and *Q. petraea* had 325 mg GAE/g extract. The collected samples were initially examined to identify the characteristics and possible applications of these substances. As illustrated in Supplementary Table S1, ellagic acid appeared as a component in the tested samples with concentrations of 1480  $\mu$ g/mL in *Q. dalechampii*, 8080  $\mu$ g/mL in *Q. frainetto*, and 4900  $\mu$ g/mL in *Q. petraea*. Another predominant compound in *Q. dalechampii* was quercetin (124  $\mu$ g/mL), while epicatechin (162  $\mu$ g/mL) was prominent in *Q. frainetto* and gallic acid (40.79  $\mu$ g/mL) stood out in *Q. petraea*. Phenolic compounds and compounds identified from *Quercus* extracts act as reducing agents in the biosynthesis process of PtNPs. By providing the necessary electrons, these compounds contribute to the reduction of platinum ions ( $\text{Pt}^{2+}$ ) to their zero-valent state ( $\text{Pt}^0$ ), thereby facilitating the biosynthesis of nanoparticles. This refers to the transformation of platinum ions from a positive oxidation state to a neutral, metallic state. In the green biosynthesis process of platinum nanoparticles, compounds in plant extracts, such as polyphenols and flavonoids, act as efficient reducing agents, donating electrons to the platinum ions and reducing them to the zero-valent state ( $\text{Pt}^0$ ). In addition to their reducing role, phenolic substances also have a role in maintaining the colloidal stability of PtNPs. Because of their chemical groups, these substances can bind to the surface of the nanoparticles, which prevents agglomeration,

keeps the nanoparticles evenly dispersed in the solution, ensuring that they remain stable for a long time. Also, components found in *Quercus* extracts can influence the shapes and sizes of PtNPs created through biosynthesis (Nasrollahzadeh *et al.* 2020; Salem *et al.* 2021).

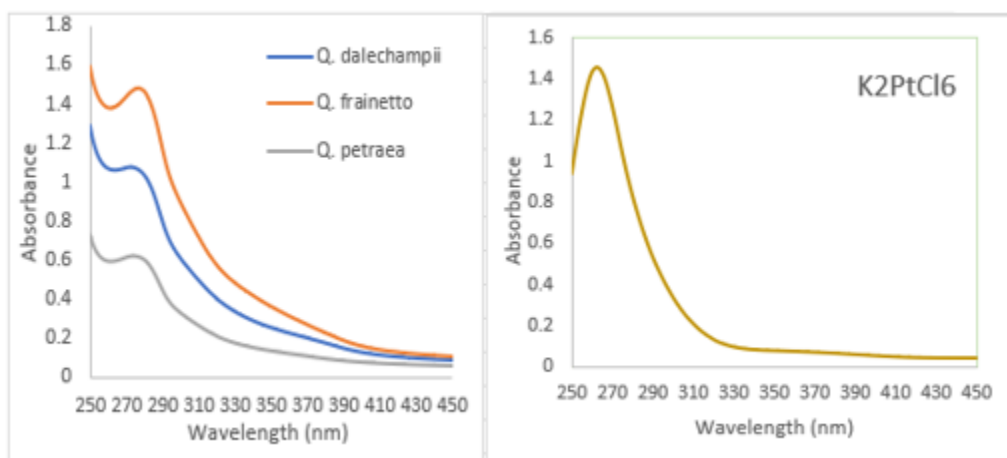


**Fig. 1.** UV spectrum of the aqueous solution of *Q. dalechampii*, *Q. frainetto*, *Q. petraea* (a) and the solution of  $K_2PtCl_6$  (b)

### Optimization of Synthesis Parameters

The formation process of QD-PtNPs, QF-PtNPs, and QP-PtNPs involved a crucial optimization step, where several parameters were investigated and adjusted. Among these parameters were included: the concentration of the  $K_2PtCl_6$  solution, the pH of the solution, the ratio of extract: $K_2PtCl_6$  solution, and the temperature of nanoparticle formation. The PtNPs formation was tracked by noting the shift in color of the mixture during the reaction. The initial light-yellow color transitioned (Fig. 2b) to dark brown (Fig. 2c) as the reaction advanced. This alteration in color signifies the transformation from Pt(IV) to Pt(II) and Pt(II) to Pt(0), indicating the creation of PtNPs. The change in color observed is believed to be linked to the surface response of Metal-NPs caused by the movement of electrons, on its surface (Nishanthi *et al.* 2019).

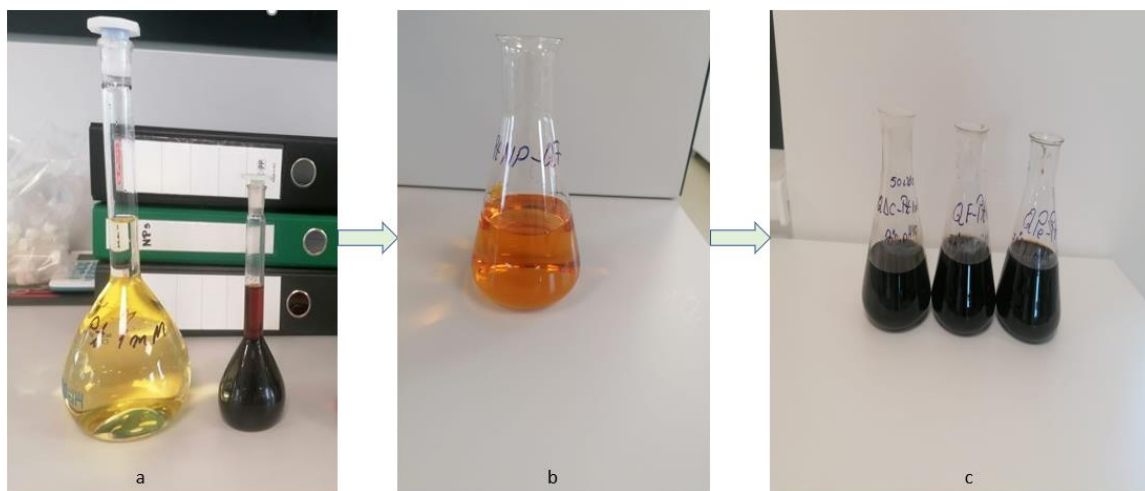


**Fig. 2.** Color shift during reaction: 1mM  $K_2PtCl_6$  solution and *Q. frainetto* extract (Fig. 2a), solution color at time T0 (Fig. 2b), color shift to dark brown as the reaction progressed (Fig. 2c)

### Determination of the Optimal Concentration of the Reducing Agent and $K_2PtCl_6$ / Extract Ratios

The first step studied in the formation of QD-PtNPs, QF-PtNPs, and QP-PtNPs determined the concentration of the  $K_2PtCl_6$  solution. Initially, 2 mL of the extract was mixed with 18 mL of  $K_2PtCl_6$  at different concentrations (0.1, 1, and 5 mM), at initial pH. Afterwards, the mixture was ultrasonicated in a bath at 70 °C for 2 h. The formation of PtNPs were validated using UV-Vis spectroscopy. The absorption spectra of the precursor platinum (Pt) salts displayed a peak at 262 nm, which occurred due to the dissociation and formation of  $2H^+$  and  $PtCl_6^{2-}$  in water (Fig. 1b). Upon introducing *Q. dalechampii*, *Q. frainetto*, and *Q. petraea* extracts, the plasmon peak of the Pt salt vanished, indicating a reduction of the Pt salt to zero valent platinum (Fig. 3). The experiments conducted indicated that using a higher concentration of  $K_2PtCl_6$  (5 mM) inhibited the synthesis process, as shown in Fig. 3. This phenomenon is due to several interdependent factors. At high concentrations, the rapid increase in nucleation can lead to the formation of a large number of nanoparticle nuclei in a very short time, causing particle aggregation due to frequent collisions between nuclei. This inhibits the formation of uniform and stable nanoparticles (Rehman *et al.* 2022). Additionally, high concentrations of platinum ions can generate an ionic screening effect, where the extra ions in the solution reduce the efficiency of reducing and stabilizing agents, slowing down or completely inhibiting the reduction process of platinum ions to zero-valent platinum atoms ( $Pt^0$ ), which are essential for nanoparticle formation (Fahmy *et al.* 2020). Similar effects were observed when using higher ratios of  $K_2PtCl_6$ /extract (1:19) as shown in Fig. 3. Therefore, it was determined that the ratio of 1:4 mL extract/mL  $K_2PtCl_6$ , at a concentration of 1 mM along with a reaction time of 2 h represented the conditions to produce QD-PtNPs and QP-PtNPs. In contrast, for QF-PtNPs biosynthesis a ratio of 1:9 mL extract/mL  $K_2PtCl_6$  at a concentration of 1 mM with a reaction time of 2 h were the suitable conditions.

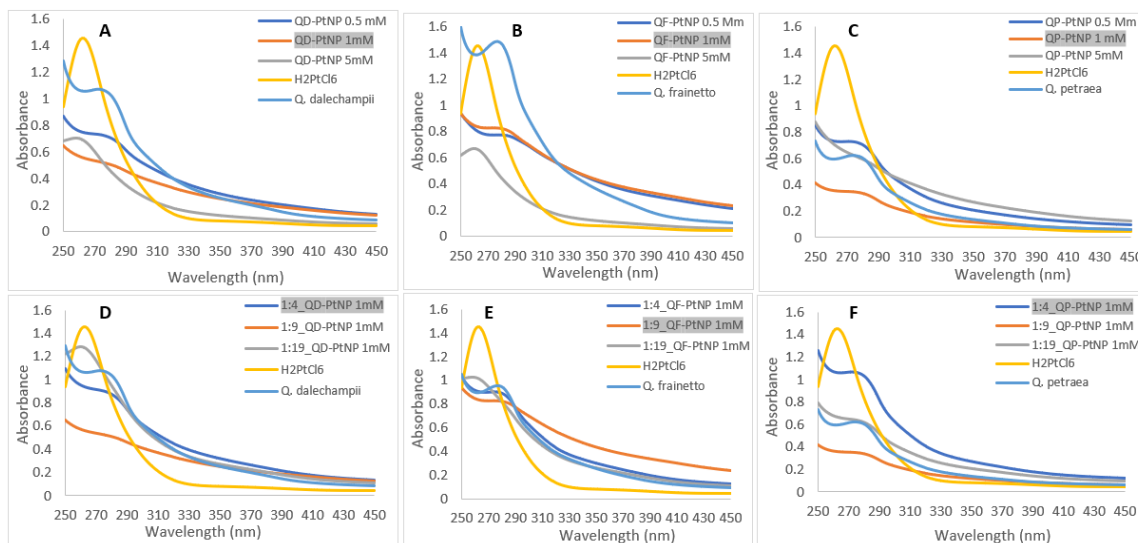


**Fig. 3.** Effect of  $K_2PtCl_6$  concentration, ratio between the volumes of plant extract, and  $K_2PtCl_6$  on the synthesis of QD-PtNPs (A, D), QF-PtNPs (B, E), and QP-PtNPs (C, F)

## Determining the Optimal Temperature and pH

After establishing the  $K_2PtCl_6$  concentration and ratio, another important factor studied in the formation of PtNPs was the solution temperature and pH. Temperature is one of the most important factors for nanoparticle synthesis of the extraction medium. The formation of PtNPs did not occur at low temperatures, and the color of the solution remained unchanged. However, a noticeable shift in color was seen as the temperature rose slowly to 70 °C. Additionally the vanishing of the peak at 260 nm suggested the creation of PtNPs (Fig. 4). As the temperature reached 80 °C, the solution clouded over and transitioned from brown to black. This change also occurred with the increased time spent in the bath, possibly indicating the aggregation of nanoparticle clusters of various sizes. The solution became turbid as the aggregated nanoparticles grew in size, leading to increased light scattering in the solution. Nanoparticle aggregation can be caused by van der Waals interactions between particles, which become more pronounced as the reaction time increases. This phenomenon is well-documented in the literature, highlighting the importance of controlling synthesis time to prevent aggregation and maintain the colloidal stability of nanoparticles (Latif *et al.* 2018; Stavinskaya *et al.* 2019). Another important factor studied in the formation of PtNPs was the pH of the solution. It plays a role in the plant mediated production of nanoparticles impacting their size, shape, and synthesis rate. The increase in pH is linked to a rise in nucleation centers formation, which influences the reduction of metal ions into metal nanoparticles. Moreover, as the pH level rises there is an increase in core center expansion and electron donation due to protonation deprotonation effects. Additionally, the solutions' pH level regulates the functionality of groups, within the plant extract, which ultimately determines how quickly metal salt reduction occurs (Jameel *et al.* 2020). The effect of pH on PtNPs synthesis was investigated at pH = 7.5; pH = 8; pH = 9, and at pH = 10. The results indicate that PtNPs formation occurred rapidly in a basic environment (pH 10) compared to a neutral solution (pH 7.5). In general, the synthesis of PtNPs increases with alkalinity levels in the dispersion medium. Thus, in the case of QD-PtNPs and QF-PtNPs pH 10 is the most favorable, in contrast, in the case of QP-PtNPs a pH 9 being the most favorable. Increasing time had no significant effect on PtNPs synthesis at different pHs, but PtNPs synthesis reached equilibrium after 2 h. The findings were supported by Nishanthi *et al.* (2019) and Soundarrajan *et al.* (2011). Nishanthi *et al.* (2019) examined how varying pH levels (4 to 8) impacted the PtNPs synthesis with *Garcinia mangostana* L. peel extract. Thus, at acidic pH (pH of 4) it led to the formation of larger PtNPs, while at alkaline pH (pH 10) it led to the formation of smaller PtNPs (Nishanthi *et al.* 2019). Soundarrajan *et al.* (2011) utilized *Ocimum sanctum* plant leaf extract for PtNPs synthesis at elevated temperatures highlighting that higher temperatures are optimal for PtNPs formation. The resulting PtNPs measured a size of 23 nm and exhibited irregular shapes (Soundarrajan *et al.* 2011).

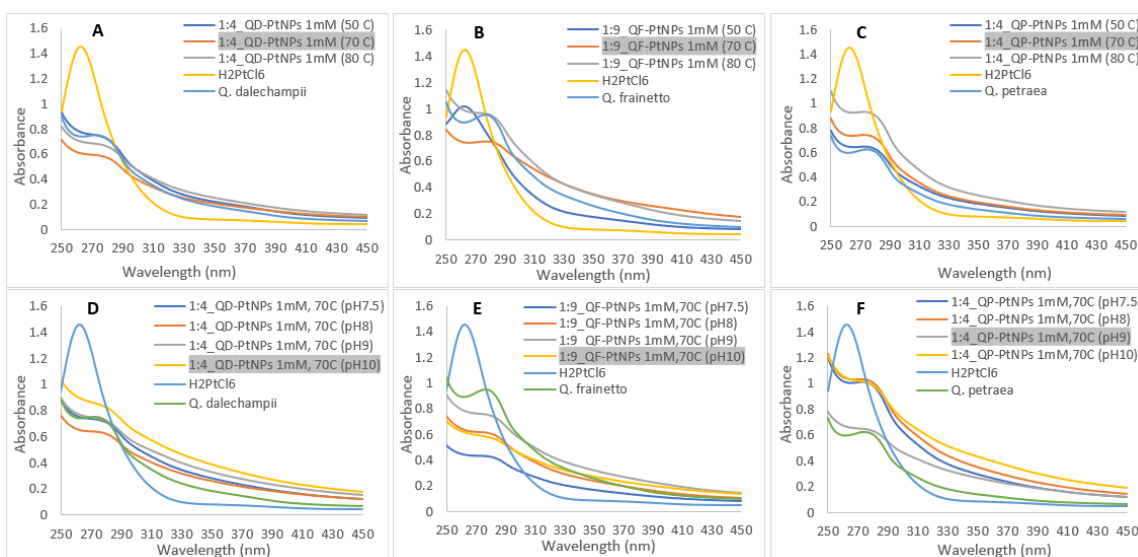


**Fig. 4.** Effect of temperature and pH on the synthesis of QD-PtNPs (A, D), QF-PtNPs (B, E), and QP-PtNPs (C, F)

Following the optimization process, three solutions of PtNPs were obtained. These solutions were: QD-PtNPs (ratio 1:4 mL extract/mL  $K_2PtCl_6$  at a concentration of 1 mM, pH 10, at 70 °C), for QF-PtNPs (ratio 1:9 mL extract/mL  $K_2PtCl_6$  at a concentration of 1 mM, pH 10, at 70 °C), and QP-PtNPs (ratio 1:4 mL extract/mL  $K_2PtCl_6$  at a concentration of 1 mM, pH 9, at 70 °C). After synthesizing the platinum nanoparticle (PtNPs) solutions, they were lyophilized to remove the water content, a process that significantly contributes to the stabilization of the chemical structure and the prevention of degradation. Lyophilization thus ensures effective preservation of the intrinsic properties of the nanoparticles. The resulting dry matter was then used for detailed assessments of biological activity, enabling accurate and reproducible analyses in laboratory studies. This method is essential for maintaining the integrity of compounds during testing and subsequent application in various biomedical fields.

### Characterization of PtNPs

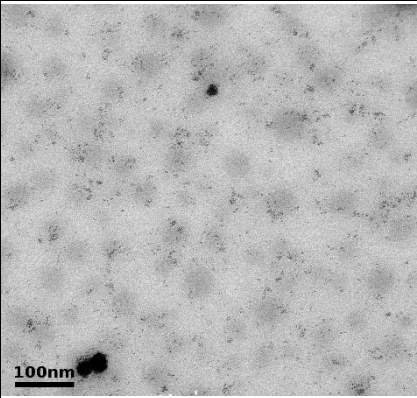
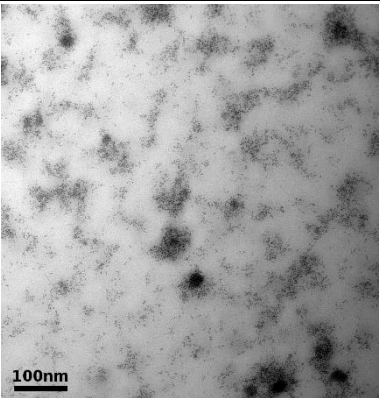
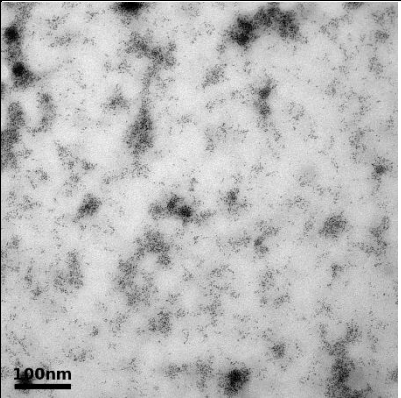
After determining the optimal conditions mentioned above, additional analytical techniques were employed to ensure the formation and quality of the PtNPs. Transmission Electron Microscopy (TEM) confirmed the morphology and uniform size of the nanoparticles. Dynamic Light Scattering (DLS) measured the size distribution and ensured colloidal stability, while Fourier Transform Infrared Spectroscopy (FTIR) verified the chemical composition and the presence of functional groups on the nanoparticle surface, confirming their stability. Additionally, the obtained PtNPs were acquired underwent an examination, during which the overall quantity of polyphenols was assessed utilizing the Folin Ciocalteu technique. Further, the substances found in *Quercus* extracts and generated during the biosynthesis of PtNPs were identified through high-performance liquid chromatography (HPLC). These investigations provided insights into the composition and characteristics of PtNPs, along with the significance of polyphenols in the biosynthesis procedure and their possible uses.

Another important role of extractive materials is to act as stabilizers for nanoparticles, preventing their collision and aggregation. In this study, the bioactive compounds present in the extracts of *Q. dalechampii*, *Q. frainetto*, and *Q. petraea*

significantly contributed to the stabilization of platinum nanoparticles (PtNPs). These compounds, such as polyphenols, tannins, and flavonoids, adsorb onto the surface of the nanoparticles, forming a protective layer that prevents their aggregation and keeps them well dispersed in solution. Efficient stabilization of nanoparticles is essential for maintaining their functional properties and ensuring optimal biological activity.

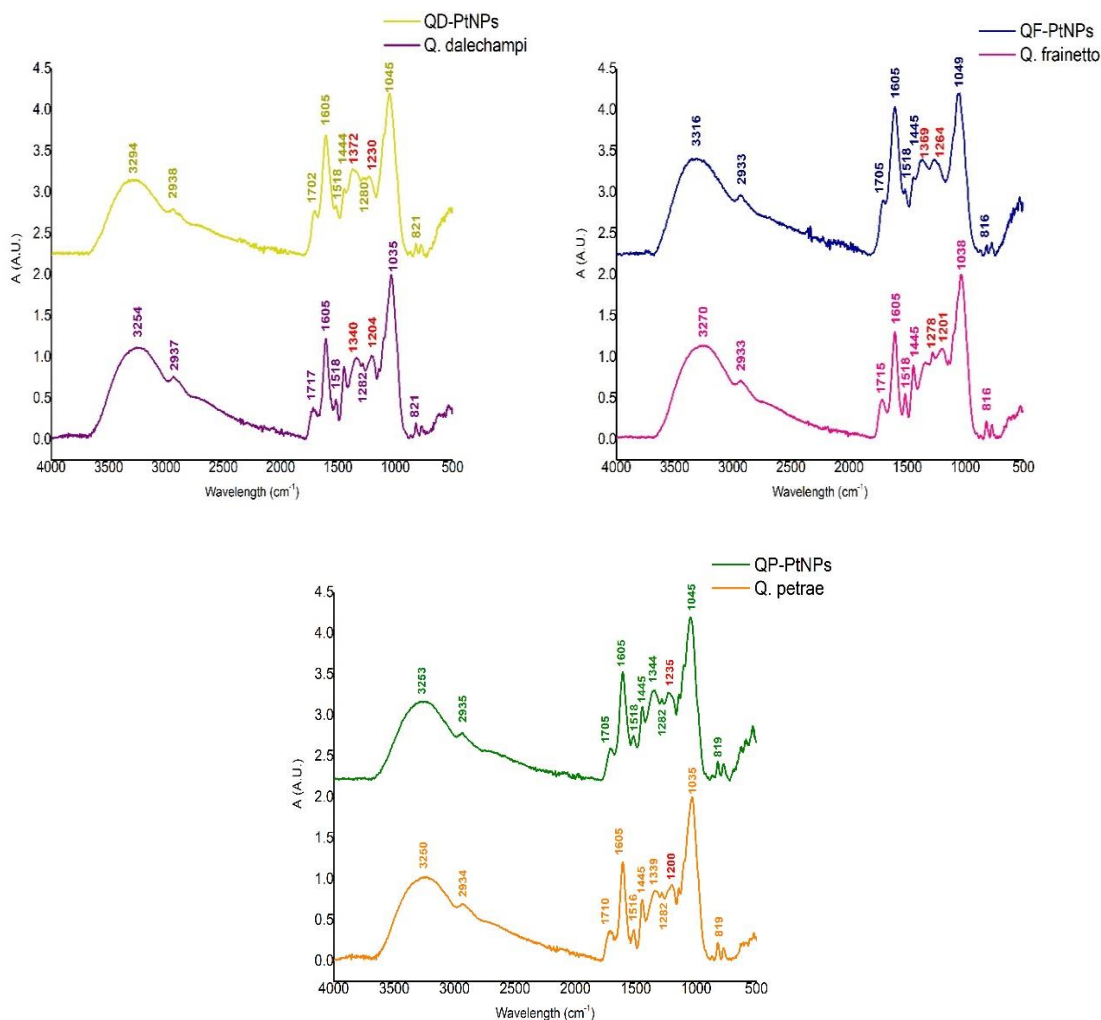
The FTIR analyses were performed to identify the biomolecules involved in the reduction of  $\text{Pt}^{2+}$  ions and the synthesis of PtNPs in the three different extracts. The FTIR spectra for each extract and the PtNPs synthesized with them are shown in Fig. 6 for a more accurate comparison and better identification of features. The observations suggest that the PtNPs synthesized using the extracts had similar chemical groups, highlighted by similar peaks in the spectra. The intense peaks between 3500 to 3200  $\text{cm}^{-1}$  (peaking at 3294  $\text{cm}^{-1}$  for QD-PtNPs, 3316  $\text{cm}^{-1}$  for QF-PtNPs, and 3253  $\text{cm}^{-1}$  for QP-PtNPs) are associated with the vibrations of O-H groups in the organic phase of the extracts, due to the abundant presence of polyphenolic structures in them (Nandiyanto *et al.* 2019). This connection suggests a correlation between PtNPs and all three *Quercus* extracts. Additionally, the peaks observed in the region 3200 to 3000  $\text{cm}^{-1}$  correspond to C-H and  $\text{CH}_2$ -,  $\text{CH}_3$ -vibrations of polysaccharides, present in significant amounts in *Quercus* extracts. The absorbance bands at: 1702  $\text{cm}^{-1}$  for QD-PtNPs, 1705  $\text{cm}^{-1}$  for QF-PtNPs, and QP-PtNPs are attributed to C=O groups, indicating an association between PtNPs and compounds, such as quercetin, epicatechin, and gallic acid, identified in *Quercus* extracts. Other observations include the presence of primary amine at 1605  $\text{cm}^{-1}$  and absorbance bands at 1518 and 1445  $\text{cm}^{-1}$  indicate aromatic compounds. In addition, the appearance of peaks at 1372 and 1230  $\text{cm}^{-1}$ , especially in QD-PtNPs, suggests their formation through the interaction of the organic extract with the metal particles. Similarly, for QF-PtNPs, the absorbance peaks at 1369 and 1264  $\text{cm}^{-1}$  indicate the synthesis process. In the case of QP-PtNPs, fewer peaks associated with reduction were observed, but the peaks at 1235  $\text{cm}^{-1}$  confirm the interaction between the *Quercus petraea* extract and the metal. These observations highlight the complexity of the interactions between organic extracts and metal particles during the synthesis of PtNPs.

Figure 5 shows the TEM images and the average sizes generated by DLS of the PtNPs. In all cases, the PtNPs show a spherical and monodisperse morphology. The dimensions of QF-PtNPs and QP-PtNPs are approximately the same ( $41.6 \pm 7.6$  nm and  $41 \pm 5.3$  nm), in contrast, the dimensions of QD-PtNPs are a bit larger, respectively  $58.5 \pm 7.6$  nm.

Platinum Nanoparticles		
Magnification: 300000x		
QD-PtNPs	QF-PtNPs	QP-PtNPs
		
Size (nm)		
58.5 ± 7.6 nm	41.6 ± 5.4 nm	41 ± 5.3 nm

**Fig. 5.** TEM images and size DLS of QD-PtNPs, QF-PtNPs, and QP-PtNPs

Polyphenols mainly contributed to the synthesis and stabilization of PtNPs. Their contribution is also supported by a significant decrease in the phenolic content of the reaction mixtures after the synthesis and separation of PtNPs. The amount of TPC of the extracts was over 300 mg GAE/g. In contrast, the amount of TPC for QD-PtNPs was 319 mg GAE/g, for QF-PtNPs it was 135 mg GAE/g, and for QP-PtNPs it was 354 mg GAE/g (Fig. 7). In addition to TPC, the substances found in *Q. dalechampii*, *Q. frainetto*, and *Q. petraea* were analyzed both before and after the biosynthesis of PtNPs using HPLC to reinforce the findings observed in FTIR and UV-Vis spectroscopy. A total of 13 reference samples were employed for this assessment (Supplementary Table S1). After the formation of nanoparticles, the compounds initially present in the extracts underwent a reduction and were transformed into PtNPs. This transformation entails a chemical reduction process, where organic compounds from plants function as reducing agents. For example, ellagic acid in the extracts was identified in the largest amount of the compounds identified. In contrast, in the PtNPs solutions, ellagic acid was undetermined. This is because the biosynthesis of PtNPs is associated with phenolic compounds, primarily with the ellagic acid (Rokade *et al.* 2018). Among the remaining compounds detected after PtNPs biosynthesis are acid, epicatechin, and taxifolin. As also observed in the PtNPs optimization step, the reduction of platinum ions was influenced by specific factors such as temperature, pH, and duration; these variables can affect both the efficacy and the size of the nanoparticles formed.



**Fig. 6.** FTIR spectrum of *Q. dalechampii*, QD-PtNPs, *Q. frainetto*, QF-PtNPs, *Q. petraea*, and QP-PtNPs

### Antioxidant Activity of PtNPs

The antioxidant potential of PtNPs obtained with oak bark extracts was evaluated by four complementary *in vitro* methods, the results of which are shown in Fig. 7. Free radical scavenging using methods, such as DPPH and ABTS, is one way to evaluate how well the compounds work as antioxidants. The stronger a substance is in scavenging radicals, the more effective it is as an antioxidant. In addition, tests such as FRAP (Ferric Ion Reduction Potential) and CUPRAC (Copper Ion Reduction Potential) measure how well a compound can reduce iron and copper ions, providing another insight into antioxidant capacity. Thus, as can be seen in Fig. 7, among the PtNPs, the strongest DPPH free radical scavenging activity was achieved by QP-PtNPs (539 mg GAE/g dw), a similar trend being observed in terms of the reducing power of ferric ions (FRAP = 783 mg GAE/g dw) and the reducing power of copper ions (CUPRAC = 573 mg GAE/g dw). In contrast, the most pronounced ABTS free radical scavenging activity was achieved by QD-PtNPs (605 mg GAE/g dw).

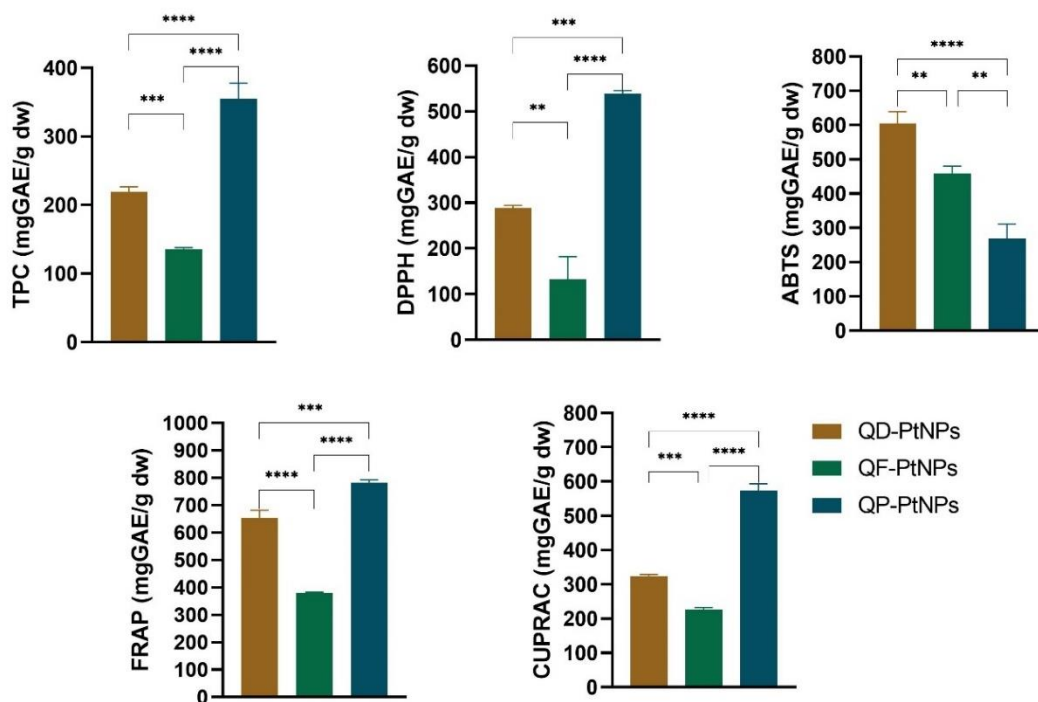


**Fig. 7.** TPC and antioxidant capacity values measured for QD-PtNPs, QF-PtNPs, and QP-PtNPs. Statistical analysis was performed by one-way ANOVA test, with Tukey's multiple comparisons post-test. All determinations were made in triplicate. Data were statistically significant where \*\*\*\* $p < 0.0001$ , \*\*\* $p < 0.0005$  and \*\* $p < 0.01$ .

The existing research backing the properties of PtNPs produced with extracts is limited. There are a few studies that at times offer conflicting conclusions about how effective these nanoparticles are as antioxidants. The DPPH free radical scavenging abilities at various concentrations of pure *Cordyceps* extract (CE) and PtNP were measured to evaluate the antioxidant activity of the synthesized PtNPs. As the sample concentration increased from 0.50  $\mu\text{g/mL}$  to 125.00  $\mu\text{g/mL}$ , the color change of the DPPH solution (from violet to light yellow) became more pronounced, and the DPPH free radical scavenging of the PtNPs increased from 27.8% to 44.0%, while the scavenging ability of CE increased from 18.4% to 25.4%. The scavenging ability of PtNPs was significantly higher than that of CE at the same concentration. Additionally, it was found that the antioxidant activity of PtNPs was positively correlated with the concentration of PtNPs (Liu *et al.* 2022). PtPdNPs showed a superior DPPH radical (56.71%  $\pm$  0.4%) and nitric oxide (47.17%  $\pm$  1.59%) scavenging activity, whereas PtNPs and PdNPs showed an average activity of capturing the DPPH radical (31.87%  $\pm$  0.29%, respectively, 27.1%  $\pm$  0.69%) and a very weak activity of capturing nitric oxide (11.11%  $\pm$  1.35%, respectively, 10.53%  $\pm$  2.54%) (Sougata Ghosh *et al.* 2015). Zhang *et al.* (2023) demonstrated the antioxidant activity of PtNPs obtained with *Nymphaea tetragona* extract, depending on the ratio of  $\text{H}_2\text{PtCl}_6$  solution and extract (L1-PtNP (1:1 ratio) and L4-PtNP (1:1 ratio)). Thus, the antioxidant activity of L4-PtNPs (IC<sub>50</sub> value is 2.98  $\pm$  0.041 g/mL) was eminently stronger than L1-PtNPs ( $p < 0.05$ ), indicating that L4-PtNPs displayed ferric ion reducing activity and free radical scavenging (ABTS) better (Zhang *et al.* 2023).

### ***In vitro* Antimicrobial Activity of PtNPs**

The PtNPs synthesized using *Q. dalechampii*, *Q. frainetto*, and *Q. petraea* (QD-PtNPs, QF-PtNPs, QP-PtNPs) were evaluated for their antibacterial activities against Gram-positive and Gram-negative pathogenic bacteria and to evaluate their antifungal activity. Table 2 shows the MIC values of PtNPs against bacterial strains and the MFC values of PtNPs against fungal strains. The PtNPs were effective against *Enterococcus faecalis* and *Escherichia coli* at a concentration of 5 mg/mL. In another study to be published, the results of the antibacterial activity of the extracts are presented. However, the extracts used in the synthesis of these nanoparticles did not show any inhibitory effect against these bacteria. The variation in results can be attributed to changes in structure and composition triggered by PtNPs. These changes may promote interactions with cell membranes, ultimately leading to disruption or suppression of bacterial proliferation. The PtNPs did not show any inhibitory effect against MSSA (except QF-PtNPs), MRSA, *Klebsiella pneumoniae*, or *Pseudomonas aeruginosa*. Comparing the results for the antibacterial activity of extracts and PtNPs, the extracts used presented lower MIC values compared to PtNPs. The reason behind this difference lies in the range of compounds and molecules in extracts as opposed to nanoparticles. These additional compounds could enhance activity either individually or synergistically with the extracted compounds. A possible explanation for why PtNPs showed higher or unclear MIC values at the tested concentrations could be attributed to the way metal ions interact with proteins and nucleic acids leading to cell death through a slower process that requires a higher amount of MNP for effective cell termination (Hussein-Al-Ali *et al.* 2014; Dong *et al.* 2018; Harun *et al.* 2021).

**Table 1.** Antimicrobial Activity of QD-PtNPs, QF-PtNPs, and QP-PtNPs in mg/mL

	QD-PtNPs	QF-PtNPs	QP-PtNPs
<i>Staphylococcus aureus</i> ATCC 25923	> 5.00	5.00	> 5.00
Methicillin-resistant <i>Staphylococcus aureus</i> ATCC 43300	> 5.00	> 5.00	> 5.00
<i>Enterococcus faecalis</i> ATCC 29212	5.00	5.00	5.00
<i>Escherichia coli</i> ATCC 25922	5.00	5.00	5.00
<i>Klebsiella pneumoniae</i> ATCC 13883	> 5.00	> 5.00	> 5.00
<i>Pseudomonas aeruginosa</i> ATCC 27853	> 5.00	> 5.00	> 5.00
<i>Candida albicans</i> ATCC 10213	> 5.00	> 5.00	> 5.00
<i>Candida krusei</i> ATCC 6258	1.25	0.63	0.16
<i>Candida auris</i> ATCC 10913	5.00	> 5.00	5.00

The PtNPs did not demonstrate any inhibitory impact on *Candida albicans*. This result can be attributed to the inability of the nanoparticles to interact effectively with this species of *Candida*. The CFM of QP-PtNP against *Candida krusei* was 0.16 mg/mL, followed by QF-PtNP at 0.63 mg/mL and QD-PtNP at 1.25 mg/mL. The variation in sensitivity could be elucidated by the differences in chemical composition, physicochemical properties of the extracts, and how the nanoparticles interact with each other. Regarding *Candida auris*, both QD-PtNPs and QP-PtNPs showed an inhibitory activity (CFM) against this species of 5 mg/mL. Thus far, there has been no research to definitively demonstrate the antifungal capabilities of PtNPs obtained using extracts. This underscores the need for further investigation to fully understand how these nanoparticles can fight infection. The size of platinum nanoparticles (PtNPs) plays a crucial role in their antimicrobial activity. Smaller nanoparticles have a larger specific surface area, enabling them to interact more effectively with microorganisms and penetrate cell membranes more

easily. Studies have shown that smaller platinum nanoparticles exhibit increased antimicrobial activity due to their larger specific surface area and enhanced ability to generate reactive oxygen species (ROS), which are lethal to bacteria. For instance, platinum nanoparticles smaller than 10 nm have demonstrated significantly higher antibacterial efficacy compared to larger ones (Fahmy *et al.* 2020; Prabhu and Gajendran 2017). Among the three PtNP solutions tested, QP-PtNPs with a size of 41 nm showed activity against *Candida krusei*. Similarly, QF-PtNPs measuring 41.6 nm also showed efficacy against both *Candida krusei* and *Candida auris*. In contrast, the QD-PtNPs with a size of 58.5 nm did not show efficacy against *Candida auris* and *Candida albicans*. These findings imply that the size of nanoparticles may influence their ability to fight fungal infections, indicating that smaller nanoparticles may be more potent against fungi. A study comparing the antifungal performance of PtNPs with currently available pharmaceutical antifungal agents was recently published. Antifungal activity of PtNP, in contrast, provided reasonable antifungal activity against harmful fungi such as *Cladosporium fulvum*, *Colletotrichum acutatum*, *Didymella bryoniae*, *Phytophthora drechsleri*, and *Phytophthora capsici* (Velmurugan *et al.* 2016). Antifungal activity of PtNPs, as reported previously, can predict that these PtNPs result in membrane damage, increased ROS generation, and change in mycelial morphology, which ultimately resulted in DNA damage or cell damage (Godugu and Rao Beedu 2018).

## CONCLUSIONS

1. The results of this study clearly indicate that the bark of *Quercus dalechampii*, *Q. frainetto*, and *Q. petraea* can be effectively used to produce bioactive platinum nanoparticles (PtNPs).
2. The PtNPs obtained from the bark extract of these oak species were well dispersed, had a spherical shape, and were small ( $58.5 \pm 7.6$  nm,  $41.6 \pm 5.4$  nm, and  $41 \pm 5.3$  nm, respectively).
3. The QP-PtNPs showed the highest 2,2-diphenyl-1-picrylhydrazyl (DPPH), ferric reducing ability of plasma (FRAP), and cupric reducing antioxidant capacity (CUPRAC) free radical scavenging activity, while QD-PtNPs showed highest 2,2'-azinobis-(3-ethylbenzothiazoline-6-sulfonic acid (ABTS) free radical scavenging activity. Moreover, the QD-PtNPs, QF-PtNPs, and QP-PtNPs showed promising antimicrobial properties, particularly effective against specific bacteria, such as *Enterococcus faecalis*, *Escherichia coli*, as well as certain candida species such as *Candida krusei* and *Candida auris*.
4. The varied efficacy observed indicates that the chemical composition, characteristics, and size of nanoparticles play roles in their antimicrobial performance. This highlights the potential of PtNPs as agents and highlights the need for further studies to enhance their efficacy against a wider range of pathogens.

## ACKNOWLEDGMENTS

This work was supported by the University of Medicine, Pharmacy, Sciences and Technology “George Emil Palade” of Târgu Mures Research grant number 10127/17/17.12.2020.

## REFERENCES CITED

- Alinaghi, M., Mokarram, P., Ahmadi, M., and Bozorg-Ghalati, F. (2024). “Biosynthesis of palladium, platinum, and their bimetallic nanoparticles using rosemary and ginseng herbal plants: Evaluation of anticancer activity,” *Scientific Reports* 14(1), article 5798. DOI: 10.1038/s41598-024-56275-z
- Babotă, M., Mocan, A., Vlase, L., Cris, O., Ielciu, I., Gheldiu, A.-M., Cristian Vodnar, D., Cris, G., and Păltinean, R. (2018). “Phytochemical analysis, antioxidant and antimicrobial activities of *Helichrysum arenarium* (L.) Moench. and *Antennaria dioica* (L.) Gaertn. flowers,” *Molecules* 23(2), article 409. DOI: 10.3390/molecules23020409
- Bendale, Y., Bendale, V., and Paul, S. (2017). “Evaluation of cytotoxic activity of platinum nanoparticles against normal and cancer cells and its anticancer potential through induction of apoptosis,” *Integrative Medicine Research* 6(2), 141-148. DOI: 10.1016/J.IMR.2017.01.006
- Bhardwaj, K., Dhanjal, D. S., Sharma, A., Nepovimova, E., Kalia, A., Thakur, S., Bhardwaj, S., Chopra, C., Singh, R., Verma, R., *et al.* (2020). “Conifer-derived metallic nanoparticles: Green synthesis and biological applications,” *International Journal of Molecular Sciences* 21(23), article 9028. DOI: 10.3390/ijms21239028
- Castro, L., Blázquez, M. L., González, F., Muñoz, J. Á., and Ballester, A. (2015). “Biosynthesis of silver and platinum nanoparticles using orange peel extract: Characterisation and applications,” *IET Nanobiotechnology* 9(5), 252-258. DOI: 10.1049/iet-nbt.2014.0063
- Chicea, D., Nicolae-Maranciuc, A., Doroshkevich, A. S., Chicea, L. M., Ozkendir, O. M. (2023). “Comparative synthesis of silver nanoparticles: Evaluation of chemical reduction procedures, AFM and DLS size analysis,” *Materials*, 16(15), article 5244. DOI: 10.3390/ma16155244
- Chicea, D., Nicolae-Maranciuc, A., and Chicea, L.-M. (2024). “Silver nanoparticles-chitosan nanocomposites: A comparative study regarding different chemical syntheses procedures and their antibacterial effect,” *Materials* 17(5), article 1113. DOI: 10.3390/ma17051113
- Coman, N.-A., Babotă, M., Nădășan, I., Dinică, Ș., Ștefănescu, R., Frumuzachi, O., Man, A., Mocan, A., and Tanase, C. (2023). “Comparative study on the chemical composition and biological activity of polyphenolic extracts obtained from *Maclura pomifera* (Raf.) C.K. Schneid bark and periderm,” *BioResources* 18(4), 8104-8119. DOI: 10.15376/biores.18.4.8104-8119
- Coman, N.-A., Nicolae-Maranciuc, A., Berta, L., Nicolescu, A., Babotă, M., Man, A., Chicea, D., Farczadi, L., Jakab-Farkas, L., Silva, B., Veiga-Matos, J., and Tanase, C. (2024). “Green synthesis of metallic nanoparticles from *Quercus* bark extracts: Characterization and functional properties,” *Antioxidants* 13, article 822. DOI: 10.3390/antiox13070822.

- Dhiman, S., Mosselhy, D., Jagtap, S., Ghosh, S., Ranpariya, B., Salunke, G., Karmakar, S., Babiya, K., Sutar, S., Kadoo, N., *et al.* (2021). “Antimicrobial synergy of silver-platinum nanohybrids with antibiotics,” *Frontiers in Microbiology* 11, article ID 610968. DOI: 10.3389/fmicb.2020.610968
- Dong, F., Yuliati, L., Reli, M., Xu, Y., Regmi, C., Joshi, B., Ray, S. K., Gyawali, G., and Pandey, R. P. (2018). “Understanding mechanism of photocatalytic microbial decontamination of environmental wastewater,” *Frontiers in Chemistry* 6, article 33. DOI: 10.3389/fchem.2018.00033
- Eltaweil, A. S., Fawzy, M., Hosny, M., Abd El-Monaem, E. M., Tamer, T. M., and Omer, A. M. (2022). “Green synthesis of platinum nanoparticles using *Atriplex halimus* leaves for potential antimicrobial, antioxidant, and catalytic applications,” *Arabian Journal of Chemistry* 15(1), article ID 103517. DOI: 10.1016/j.arabjc.2021.103517
- Fahmy, S. A., Preis, E., Bakowsky, U., Mohamed, H., and Azzazy, E.-S. (2020). “Platinum nanoparticles: Green synthesis and biomedical applications,” *Molecules* 25, article 4981. DOI: 10.3390/molecules25214981.
- Ghosh, S., Nitnavare, R., Dewle, A., Tomar, G. B., Chippalkatti, R., More, P., Kitture, R., Kale, S., Bellare, J., and Chopade, B. A. (2015). “Novel platinum–palladium bimetallic nanoparticles synthesized by *Dioscorea bulbifera*: Anticancer and antioxidant activities,” *International Journal of Nanomedicine*, article 7477-7490. DOI: 10.2147/IJN.S91579.
- Godugu, D., and Beedu, S. R. (2018). “Biopolymer-mediated synthesis and characterisation of platinum nanocomposite and its anti-fungal activity against *A. parasiticus* and *A. flavus*,” *Micro & Nano Letters* 13(10), 1491-1496. DOI: 10.1049/mnl.2018.5097
- Gupta, K., and Chundawat, T. S. (2019). “Bio-inspired synthesis of platinum nanoparticles from fungus *Fusarium oxysporum*: Its characteristics, potential antimicrobial, antioxidant and photocatalytic activities,” *Materials Research Express* 6(10), article ID 1050d6. DOI: 10.1088/2053-1591/ab4219
- Harun, A. M., Farid, N., Noor, M., Zaid, A., Yusoff, M. E., Shaari, R., Affandi, D. N., Fadil, F., Azizi, M., Rahman, A., *et al.* (2021). “The antimicrobial properties of nanotitania extract and its role in inhibiting the growth of *Klebsiella pneumonia* and *Haemophilus influenza*,” *Antibiotics* 10(8), article 961. DOI: 10.3390/antibiotics10080961
- Hussein-Al-Ali, S. H., El Zowalaty, M. E., Hussein, M. Z., Geilich, B. M., and Webster, T. J. (2014). “Synthesis, characterization, and antimicrobial activity of an ampicillin-conjugated magnetic nanoantibiotic for medical applications,” *International Journal of Nanomedicine* 9, 3801-3814. DOI: 10.2147/ijn.s61143
- Jameel, M. S., Abdul Aziz, A., and Dheyab, M. A. (2020). “Green synthesis: Proposed mechanism and factors influencing the synthesis of platinum nanoparticles,” *Green Processing and Synthesis* 9(1), 386-398. DOI: 10.1515/gps-2020-0041
- Jiao, Y., Wang, X., and Chen, J. (2021). “Biofabrication of AuNPs using *Coriandrum sativum* leaf extract and their antioxidant, analgesic activity,” *Science of The Total Environment* 767, article ID 144914. DOI: 10.1016/j.scitotenv.2020.144914
- Karim, N. A., Rubinsin, N. J., Burukan, M. A. A., and Kamarudin, S. K. (2019). “Sustainable route of synthesis platinum nanoparticles using orange peel extract,” *International Journal of Green Energy* 16(15), 1518-1526. DOI: 10.1080/15435075.2019.1671422
- Latif, M. S., Kormin, F., Mustafa, M. K., Mohamad, I. I., Khan, M., Abbas, S., Ghazali, M. I., Shafie, N. S., Bakar, M. F. A., Sabran, S. F., and Fuzi, S. F. Z. M. (2018).

- “Effect of temperature on the synthesis of *Centella asiatica* flavonoids extract-mediated gold nanoparticles: UV-visible spectra analyses,” AIP Conf Proc 2016. *American Institute of Physics Inc.* DOI: 10.1063/1.5055473.
- Liu, L., Jing, Y., Guo, A., Li, X., Li, Q., Liu, W., and Zhang, X. (2022). “Biosynthesis of platinum nanoparticles with *Cordyceps* flower extract: Characterization, antioxidant activity and antibacterial activity,” *Nanomaterials* 12(11), article ID 1904. DOI: 10.3390/nano12111904
- Marvi, P. K., Ahmed, S. R., Das, P., Ghosh, R., Srinivasan, S., and Rajabzadeh, A. R. (2024). “*Prunella vulgaris*-phytosynthesized platinum nanoparticles: Insights into nanozymatic activity for H<sub>2</sub>O<sub>2</sub> and glutamate detection and antioxidant capacity,” *Talanta* 274, article ID 125998. DOI: 10.1016/j.talanta.2023.125998
- Nandiyanto, A. B. D., Oktiani, R., and Ragadhita, R. (2019). “How to read and interpret FTIR spectroscopy of organic material,” *Indonesian Journal of Science and Technology* 4(1), 97-118. DOI: 10.17509/ijost.v4i1.15806
- Nasrollahzadeh, M., Sajjadi, M., Dadashi, J., and Ghafari, H. (2020). “Pd-based nanoparticles: Plant-assisted biosynthesis, characterization, mechanism, stability, catalytic and antimicrobial activities,” *Advances in Colloid and Interface Science* 276, article ID 102103. DOI: 10.1016/j.cis.2019.102103
- Nishanthi, R., Malathi, S., and Palani, P. (2019). “Green synthesis and characterization of bioinspired silver, gold and platinum nanoparticles and evaluation of their synergistic antibacterial activity after combining with different classes of antibiotics,” *Materials Science and Engineering: C* 96, 693-707. DOI: 10.1016/j.msec.2018.11.050
- Özyürek, M., Güçlü, K., Tütem, E., Sözgen Başkan, K., Erçağ, E., Çelik, S. E., Baki, S., Yıldız, L., Karaman, Ş., and Apak, R. (2011). “A comprehensive review of CUPRAC methodology,” *Analytical Methods* 3(11), 2439-2453. DOI: 10.1039/c1ay05320e
- Ponsanti, K., Tangnorawich, B., Natphopsuk, S., Toommee, S., and Pechyen, C. (2024). “Physicochemical aspects of platinum nanoparticles (PtNPs) from biological synthesis: Influence of plant leaf based extracts as the reducing agent,” *International Journal of Precision Engineering and Manufacturing-Green Technology* 1097-1113. DOI: 10.1007/s40684-023-00592-7
- Prabhu, N., and Gajendran, T. (2017). “Green synthesis of noble metal of platinum nanoparticles from *Ocimum sanctum* (Tulsi) plant-extracts,” *IOSR Journal of Biotechnology and Biochemistry* 3(1), 107-112. DOI: 10.9790/264X-0301107112.
- Rehman, K. U., Gouda, M., Zaman, U., Tahir, K., Khan, S. U., Saeed, S., Khojah, E., El-Beltagy, A., Zaky, A. A., Naeem, M., *et al.* (2022). “Optimization of platinum nanoparticles (PtNPs) synthesis by acid phosphatase mediated eco-benign combined with photocatalytic and bioactivity assessments,” *Nanomaterials* 12(7), article 1079. DOI: 10.3390/nano12071079.
- Rokade, S. S., Joshi, K. A., Mahajan, K., Patil, S., Tomar, G., Dubal, D. S., Parihar, V. S., Kitture, R., Bellare, J. R., and Ghosh, S. (2018). “*Gloriosa superba* mediated synthesis of platinum and palladium nanoparticles for induction of apoptosis in breast cancer,” *Bioinorganic Chemistry and Applications*, article 4924186. DOI: 10.1155/2018/4924186.
- Salem, M. Z. M., Mervat, E.-H., Ali, H. M., Abdel-Megeed, A., El-Settawy, A. A., Böhm, M., Mansour, M. M. A., and Salem, A. Z. M. (2021). “Plants-derived bioactives: Novel utilization as antimicrobial, antioxidant and phyto-reducing agents

- for the biosynthesis of metallic nanoparticles,” *Microbial Pathogenesis* 158, article ID 105107. DOI: 10.1016/j.micpath.2021.105107
- Siddiqi, K. S., Husen, A., and Rao, R. A. K. (2018). “A review on biosynthesis of silver nanoparticles and their biocidal properties,” *Journal of Nanobiotechnology* 16, article 14. DOI: 10.1186/s12951-018-0334-5
- Soundarrajan, C., Sankari, A., Dhandapani, P., Maruthamuthu, S., Ravichandran, S., Sozhan, G., and Palaniswamy, N. (2012). “Rapid biological synthesis of platinum nanoparticles using *Ocimum sanctum* for water electrolysis applications,” *Bioprocess and Biosystems Engineering* 35, 827-833. DOI: 10.1007/s00449-011-0666-0
- Stavinskaya, O., Laguta, I., Fesenko, T., and Krumova, M. (2019). “Effect of temperature on green synthesis of silver nanoparticles using *Vitex agnus-castus* extract,” *Chemistry Journal of Moldova* 14(2), 117-121. DOI: 10.19261/cjm.2019.636.
- Tanase, C., Babotă, M., Nișca, A., Nicolescu, A., Ștefănescu, R., Mocan, A., Farczadi, L., Mare, A. D., Ciurea, C. N., and Man, A. (2023). “Potential use of *Quercus dalechampii* Ten. and *Q. frainetto* Ten. barks extracts as antimicrobial, enzyme inhibitory, antioxidant and cytotoxic agents,” *Pharmaceutics* 15(2), article ID 343. DOI: 10.3390/pharmaceutics15020343
- Tanase, C., Berta, L., Coman, N. A., Roșca, I., Man, A., Toma, F., Mocan, A., Nicolescu, A., Jakab-Farkas, L., Biró, D., *et al.* (2019). “Antibacterial and antioxidant potential of silver nanoparticles biosynthesized using the spruce bark extract,” *Nanomaterials* 9(11), article ID 1541. DOI: 10.3390/nano9111541
- Tanase, C., Berta, L., Mare, A., Man, A., Talmaciu, A. I., Roșca, I., Mircia, E., Volf, I., and Popa, V. I. (2020). “Biosynthesis of silver nanoparticles using aqueous bark extract of *Picea abies* L. and their antibacterial activity,” *European Journal of Wood and Wood Products* 78, 281-291. DOI: 10.1007/s00107-020-01502-3
- Tanase, C., Cosarca, S., Toma, F., Mare, A., Cosarca, A., Man, A., Miklos, A., and Imre, S. (2018). “Antibacterial activities of spruce bark (*Picea abies* L.) extract and its components against human pathogens,” *Revista de Chimie* 69, 1462-1467
- Tsiripidis, I., and Athanasiadis, N. (2003). “Contribution to the knowledge of the vascular flora of NE Greece: Floristic composition of the beech (*Fagus sylvatica* L.) forests in the Greek Rodopi,” *Willdenowia* 33(2), 273-297. DOI: 10.3372/wi.33.33207
- Velmurugan, P., Shim, J., Kim, K., and Oh, B.-T. (2016). “*Prunus* × *yedoensis* tree gum mediated synthesis of platinum nanoparticles with antifungal activity against phytopathogens,” *Materials Letters* 174, 61-65. DOI: 10.1016/j.matlet.2016.03.069
- Zhang, Y., Cheng, S., Jia, H., Zhou, J., Xi, J., Wang, J., Chen, X., and Wu, L. (2023). “Green synthesis of platinum nanoparticles by *Nymphaea tetragona* flower extract and their skin lightening, antiaging effects,” *Arabian Journal of Chemistry* 16(1), article ID 104391. DOI: 10.1016/j.arabjc.2022.104391

Article submitted: May 30, 2024; Peer review completed: July 11, 2024; Revised version received: July 23, 2024; Accepted: September 13, 2024; Published: September 25, 2024. DOI: 10.15376/biores.19.4.8621-8641

## APPENDIX

### Supplementary Information

**Table S1.** Concentration of the Main Phytoconstituents Identified in Extracts in PtNPs as Determined and Calculated from HPLC Chromatograms, at 280 nm

Compound	Compound Concentration ( $\mu\text{g/mL}$ )						
	RT (min)	Q. <i>dalechampii</i>	Q. <i>frainetto</i>	Q. <i>petraea</i>	QD-PtNPs	QF-PtNPs	QP-PtNPs
Gallic acid	2.96	14.81	9.37	40.79	n.d.	n.d.	n.d.
Eleutheroside B	4.89	13.98	65.74	1.50	n.d.	0.07	n.d.
Chlorogenic acid	4.94	3.19	1.37	0.64	0.11	0.03	0.02
Catechin	4.97	30.02	12.38	1.50	0.49	n.d.	n.d.
Epicatechin	5.76	72.17	161.54	36.99	0.40	0.35	0.21
Luteolin-3',7-di-O--glucoside	5.90	8.99	6.38	2.04	n.d.	n.d.	n.d.
Caffeic acid	6.01	12.63	19.81	n.d.	n.d.	n.d.	n.d.
Vanillic acid	6.04	10.16	n.d.	5.18	n.d.	0.13	n.d.
Luteolin-7-O-glucoside	6.89	130.62	71.08	n.d.	n.d.	n.d.	n.d.
Ellagic acid	7.18	1477.26	8077.98	4902.84	n.d.	n.d.	n.d.
Sinapic acid	7.95	3.13	n.d.	0.71	n.d.	0.02	n.d.
Taxifolin	8.05	4.90	16.06	0.11	0.30	0.03	0,05
Quercetin	10.63	123.90	21.20	14.65	18.90	n.d.	n.d.

n.d.—not detected